The optical activity of β,γ-enones in ground and excited states using circular dichroism and circularly polarized luminescence

Magdalena Pecul*[ab] and Kenneth Ruud[b]

Received 12th July 2010, Accepted 26th August 2010
DOI: 10.1039/c0cp01149e

The circularly polarized luminescence (CPL) and electronic circular dichroism (CD) spectroscopic parameters corresponding to the $n \leftarrow \pi^*$ and $n \rightarrow \pi^*$ transitions, respectively, have been calculated for selected β,γ-enones using density functional theory. For the smallest β,γ-enone, (1*R*,4*R*)-bicyclo[2.2.1]hept-5-en-2-one (norbornenone), coupled-cluster calculations have also been carried out. The excited-state potential energy surface for three of the five enones studied reveals two minima with different C=O···C=C dihedral angles, and with rotatory strengths of opposite sign. The relative energies of the minima determine the sign of the CPL intensity, which may be the same or opposite as in the CD spectrum, in agreement with experimental data. The results obtained in this first computational study of CPL demonstrate its usefulness as an indicator of excited-state structures of chiral species.

I. Introduction

Circularly polarized luminescence (CPL) measures the differential emission of left and right circularly polarized light by a chiral sample, and can therefore be regarded as the emission spectroscopic counterpart to electronic circular dichroism (CD). When the structures of the ground and excited states are similar, the absorption band (in the CD spectrum) and the emission band (in the CPL spectrum) have the same sign and similar magnitude, due to the fact that the rotatory strengths for the ground- and excited-state geometries are similar. However, when the equilibrium structure of the electronically excited state differs significantly from the ground state geometry and the excited state has a lifetime long enough to allow the molecule to structurally relax, the CD and CPL bands are dissimilar, even to the extent of having opposite signs. CPL is thus a unique method of probing chiral molecules in their excited states.

Most contemporary applications of CPL study chiral metal (mostly lanthanide) complexes,[1,2] but in the past there was also a number of measurements of CD and CPL spectra reported for small chiral organic molecules,[3–5] including β,γ-enones.[4] We have found the results obtained for the latter of particular interest, because of the sign variations observed between the CD and CPL bands corresponding to transitions between the *n* and π* orbitals for some of these compounds. In order to understand the origin of these variations in the relative sign of the CD and CPL signals and to verify the conclusions reached on the excited-state geometries drawn on the basis of the experimental spectra, we have carried out a series of *ab initio* calculations on the β,γ-enones, shown in Fig. 1.

Evaluation of CPL spectra requires the calculation of the energy minimum on the potential energy surface (thus excited-state geometry gradients) and of the rotatory strength. This has not been possible for chiral molecules of chemical interest before the development of density functional response theory.[6,7] The present work, employing this formalism, is the first attempt to simulate CPL spectra by *ab initio* methods.

II. Theory and computational details

A Theory of CD and CPL calculations

CD spectroscopy is based on the phenomenon of differential absorption of left and right circularly polarized light by a chiral sample. For a sample of randomly oriented molecules, the difference between the absorption coefficients of left and right circularly polarized light for a transition from the ground electronic state to the *n*th excited electronic state is proportional to the scalar rotatory strength ${}^nR$, which can be obtained as a scalar product of the electric dipole and magnetic dipole transition moments. CPL is an analogous phenomenon in

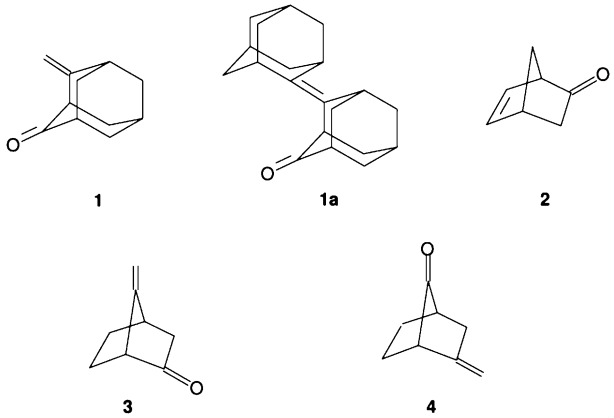

Fig. 1 The molecules under study: **1**—(1*S*,3*R*)-4-methyleneadamantan-2-one, **1a**—(1*S*,3*R*)-4-adamantylideneadamantan-2-one, **2**—(1*R*,4*R*)-bicyclo[2.2.1]hept-5-en-2-one, **3**—(1*R*)-7-methylenebicyclo[2.2.1]heptan-2-one, **4**—(1*S*)-2-methylenebicyclo[2.2.1]heptan-7-one.

[a] *Faculty of Chemistry, University of Warsaw, Pasteura 1, 02-093 Warszawa, Poland. E-mail: mpecul@chem.uw.edu.pl*
[b] *Centre for Theoretical and Computational Chemistry, Department of Chemistry, University of Tromsø, N-9037 Tromsø, Norway*

emission spectroscopy, and the CPL intensity is therefore also proportional to the rotational strength, but evaluated for the excited state geometry.

In linear response theory, the scalar rotatory strength is calculated as a residue of the linear response function.[8,9] For a transition from the ground state $|0\rangle$ to an excited state $|n\rangle$ (or the other way around), the rotatory strength is in the velocity and length gauges given by, respectively,

$$ {}^{n}R^{v} = \frac{1}{2\omega_n}\langle 0|\mathbf{p}|n\rangle \cdot \langle n|\mathbf{L}|0\rangle = \frac{1}{2\omega_n}\mathrm{Tr}\left\{ \lim_{\omega\to\omega_n} (\omega-\omega_n)\langle\langle \mathbf{p};\mathbf{L}\rangle\rangle_{\omega} \right\}, \quad (1) $$

$$ {}^{n}R^{r} = -\frac{i}{2}\langle 0|\mathbf{r}|n\rangle \cdot \langle n|\mathbf{L}|0\rangle = \mathrm{Tr}\left\{ \lim_{\omega\to\omega_n} (\omega-\omega_n)\langle\langle \mathbf{r};\mathbf{L}\rangle\rangle_{\omega} \right\}. \quad (2) $$

In these expressions atomic units are used, **r**, **p**, and **L** are the electronic position, momentum and orbital angular momentum operators, respectively; $\hbar\omega_n$ is the excitation energy for the nth electronic transition, and $\langle\langle ;\rangle\rangle$ denotes the linear response function.[8] In the length gauge, the results obtained in a finite orbital basis depend on the choice of the gauge origin. For variational methods (including DFT), this problem can be overcome by using London atomic orbitals (gauge including atomic orbitals, GIAOs).[10]

The absorption intensity for a transition from the ground state $|0\rangle$ to an excited state $|n\rangle$ is proportional to the scalar dipole strength, which can be evaluated in the velocity, length, or mixed velocity-length gauges as

$$ {}^{n}D^{v} = \frac{1}{\omega_n^2}\langle 0|\mathbf{p}|n\rangle \cdot \langle n|\mathbf{p}|0\rangle = \frac{1}{\omega_n^2}\mathrm{Tr}\left\{ \lim_{\omega\to\omega_n} (\omega-\omega_n)\langle\langle \mathbf{p};\mathbf{p}\rangle\rangle_{\omega} \right\}, \quad (3) $$

$$ {}^{n}D^{r} = \langle 0|\mathbf{r}|n\rangle \cdot \langle n|\mathbf{r}|0\rangle = \mathrm{Tr}\left\{ \lim_{\omega\to\omega_n} (\omega-\omega_n)\langle\langle \mathbf{r};\mathbf{r}\rangle\rangle_{\omega} \right\}, \quad (4) $$

$$ {}^{n}D^{vr} = \frac{1}{\omega_n}\langle 0|\mathbf{p}|n\rangle \cdot \langle n|\mathbf{r}|0\rangle = \frac{1}{\omega_n}\mathrm{Tr}\left\{ \lim_{\omega\to\omega_n} (\omega-\omega_n)\langle\langle \mathbf{p};\mathbf{r}\rangle\rangle_{\omega} \right\}. \quad (5) $$

To convert the dipole and rotatory strengths from atomic units to the cgs units employed in the experimental paper,[4] the calculated quantities are multiplied by $(eca_0)^{-2} \times 10^6$ and by $e^2ca_0\hbar m_e^{-1} \times 10^4$, respectively. Finally, we note that the absorption and emission dissymmetry factors g_a and g_e are defined, in accordance with ref. 4, as

$$ g_a = \frac{R_a}{4D_a} \quad (6) $$

$$ g_e = \frac{R_e}{4D_e}. \quad (7) $$

B Computational details

The B3LYP functional has been used for the ground- and excited-state geometry optimizations. Deficiencies of the standard exchange–correlation functionals in rendering excitation energies (and thus geometric structures of a molecule in the excited state) are well known,[11–13] but due to limitations in our programs, we have not been able to use the Coulomb-attenuated B3LYP functional (CAM-B3LYP) for the excited-state geometry optimization. The qualities of the CAM-B3LYP[14] functional for describing charge-transfer excited states is well documented,[12,13] but B3LYP in general also performs well for transitions to valence states such as the ones studied here, and we therefore do not believe the use of B3LYP for the excited-state geometry optimizations to be a serious limitation in the methodology we use. Still, we have calculated excitation energies and rotatory strengths (in the ground- and excited-state geometries) also using the CAM-B3LYP functional[12,14] in order to verify the quality of the B3LYP results. The calculations for the smallest enone (molecule **2**) have also been repeated using the coupled-cluster CC2 method[15] (the core 1s orbitals of C and O have been kept frozen). The resolution-of-the-identity (RI) approximation (RI-CC2)[16] was used for the geometry optimization of **2** for these coupled-cluster calculations.

The ground- and excited-state geometries have been calculated using the aug-cc-pVDZ basis set. Some calculations of excitation energies and rotatory strengths have also been carried out using the d-aug-cc-pVDZ and aug-cc-pVTZ basis sets,[17–20] in order to check the effect of an enlargement of the basis set on the calculated spectroscopic parameters. The DFT rotatory strengths have been calculated in the length-gauge formulation, employing London atomic orbitals (GIAOs)[10] in order to ensure independence of the results with respect to the choice of gauge origin.[9,21] Selected velocity-gauge results are shown for a more direct comparison with the CC results.

The ground-state structures, dipole strengths, and rotatory strengths have been computed using the DALTON[22] program. The TURBOMOLE[23] program has been used for the excited-state geometry optimizations.

III. Results and discussion

A Geometry of the ground and excited states

The calculated ground- and $n \rightarrow \pi^*$ excited-state structures of molecules **1**, **1a**, **2**, **3**, and **4** are shown in Fig. 2 together with the values of the improper dihedral angle ϕ(C═O···C═C) and the dihedral angle θ(═C–C–C═O). The C(C═O)C moiety, flat in the ground state, puckers either towards the C═C double bond or in the opposite direction following the $n \rightarrow \pi^*$ excitation, which may result in two minima for the excited state. This is the case for three of the systems considered (molecule **1**, **3** and **4**), where the geometry optimization on the excited-state potential energy surface revealed two minima (denoted **E1** and **E2**) with different relative arrangements of the C═O and C═C bonds (and thus different signs of the ψ angle). The structures denoted **E1** have the C═O group inclined away from the C═C bond, while the structures denoted **E2** have the C═O group inclined towards the C═C bond. For the excited state of molecule **2** and molecule **1a**, we have only found one minimum, with the C═O bond inclined away from the C═C bond (thus formally of the **E2** type).

The energies of the excited-state structures relative to the ground-state minimum are reported in Table 1.

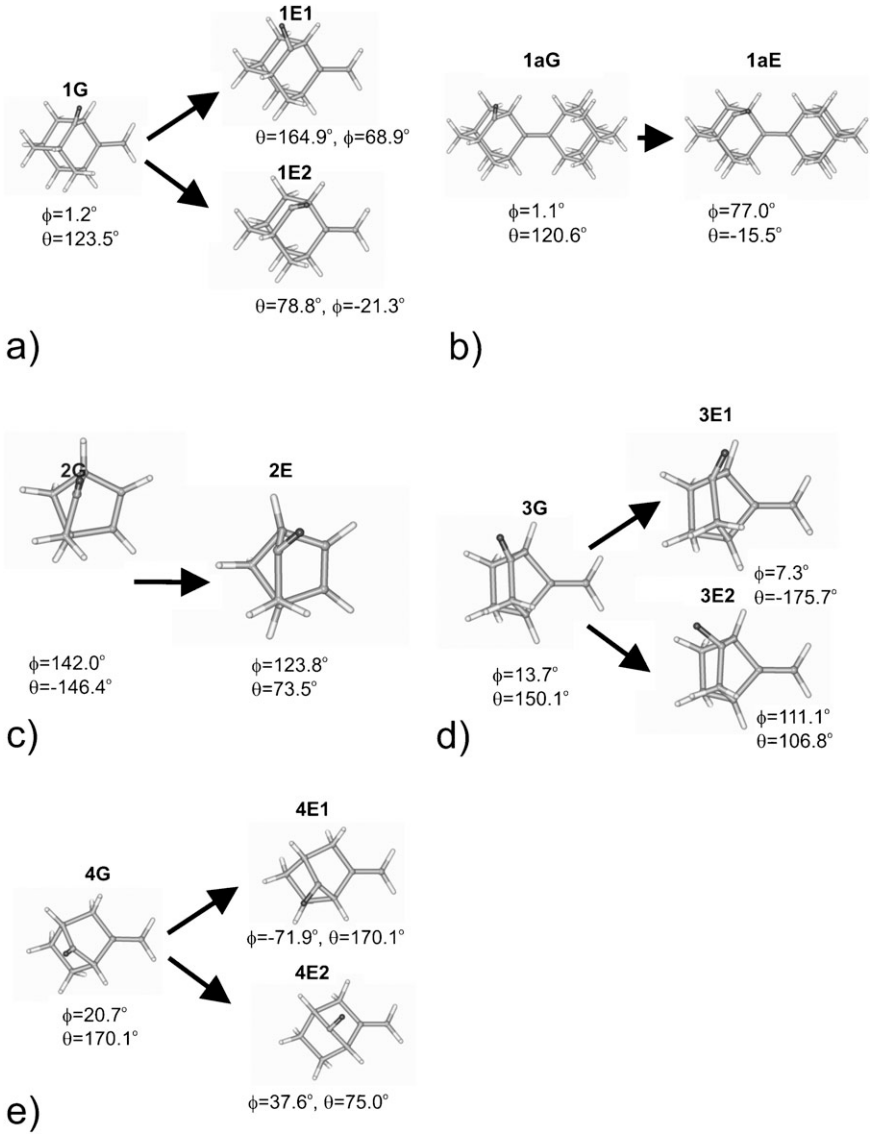

Fig. 2 The optimized structures of ground and excited state of (a) (1*S*,3*R*)-4-methyleneadamantan-2-one (**1**), (b) (1*S*,3*R*)-4-adamantylideneadamantan-2-one (**1a**), (c) (1*R*,4*R*)-bicyclo[2.2.1]hept-5-en-2-one (**2**), (d) (1*R*)-7-methylenebicyclo[2.2.1]heptan-2-one (**3**), (e) (1*S*)-2-methylenebicyclo[2.2.1]heptan-7-one (**4**) with the dihedral angles ϕ(C═O···C═C) and θ(═C–C–C═O) marked. **G** denotes ground state and **E** excited state structure. The structures denoted **E1** have the C═O group inclined away from the C═C bond, while the structures denoted **E2** have the C═O group inclined towards the C═C bond.

The CAM-B3LYP energies have been calculated for the B3LYP optimized structures. The B3LYP and CAM-B3LYP results differ, the B3LYP energies being consistently lower by roughly 0.18 eV (0.15–0.23 eV) for all the excitation energies. This difference is within the expected relative accuracy of the B3LYP and CAM-B3LYP methods for valence excitations.[12] However, both functionals indicate that the energy differences between the two excited-state minima, where present, are small (0.02 to 0.06 eV). For molecules **1** and **4**, the ordering of the excited-state structures **E1** and **E2** is reversed at the B3LYP and CAM-B3LYP levels: B3LYP calculations yield in all cases that the structure **E1** is the lowest in energy, while calculations of the CAM-B3LYP energy for the B3LYP structure predict the structure **E2** to be lower for **1** and **4** and **E1** to be lower only for **3**. This has serious consequences for the prediction of the optical response from the excited state, as we will show later on.

Table 1 The energy (in eV) of the $n \rightarrow \pi^*$ excited state relative to the ground state energy. aug-cc-pVDZ results

	B3LYP	CAM-B3LYP
1E1	3.69	3.88
1E2	3.71	3.86
1aE	3.64	3.86
2E	3.62	3.80
3E1	3.75	3.90
3E2	3.79	3.94
4E1	3.50	3.73
4E2	3.56	3.71

The RI-CC2 optimization of the excited state of **2** led to a structure similar to that obtained by the B3LYP functional, but with a much longer C═O bond (1.3595 Å for CC2, 1.2666 Å for DFT/B3LYP). There are no experimental data for the

geometry of the first excited state of **2**, but the accuracy of these numbers can be assessed by comparison of the results of CC2 and DFT/B3LYP excited-state geometry optimizations for the C=O bond length of the $^1A''$ state of formaldehyde (C_s symmetry), for which the experimental geometry is available.[24,25] The CC2/aug-cc-pVDZ geometry optimization results in a C=O bond length of 1.3773 Å for the $^1A''$ state of formaldehyde, while B3LYP/aug-cc-pVDZ yields 1.2992 Å, to be compared with the experimental bond length (r_e, derived from rotational data) of 1.3232(30) Å. Thus, CC2 tends to overestimate the carbonyl bond length in the $n \rightarrow \pi^*$ excited state, while B3LYP underestimates it (although less significantly). If we assume the trends observed for formaldehyde to hold also for the C=O bond length in the enones, the actual bond length for the $n \rightarrow \pi^*$ excited state of **2** can be estimated to be approximately 1.295 Å.

B Chiroptical parameters in the ground and excited states

1 Chiroptical parameters for the ground-state equilibrium geometries. The chiroptical parameters calculated using the CAM-B3LYP exchange–correlation functional and the aug-cc-pVDZ basis set for the ground- and excited-state structures are tabulated in Table 2 together with the experimental data of ref. 4.

For the ground-state structures (denoted **G**), the calculated rotatory strengths of the $n \rightarrow \pi^*$ transitions are in good agreement with experiment, whilst the dissymmetry factors g are less so. The latter observation is in most cases due to the fact that the rotatory strength is overestimated in the DFT calculations, while the dipole strength is underestimated, resulting in large errors in the dissymmetry factors, since they are proportional to the ratio between the rotatory and dipole strengths (see eqn (6) and (7)).

The vertical transition energies are listed in Table 2 for the sake of completeness, although Schippers, van der Ploeg and Dekkers[4] only give the approximate position of the absorption bands (33 000 cm^{-1}, corresponding to 4.1 eV). The calculated vertical excitation energies are similar for all the enones studied here, and close to this value.

It is interesting to consider the CPL parameters (calculated for excited-state structures **E1** and **E2**; see Fig. 2). It has been established experimentally[4] that the sign of the CPL band is different from that of the CD band for molecules **1**, **1a** and **4** (although in the case of **4**, the CPL spectrum is very weak and the value of g_e can at best be considered a conjecture), but remains the same for molecules **2** and **3**. Schippers *et al.*[4] concluded, on the basis of the evidence they had collected from CD spectra of enones with known ground-state geometries,[26] that it is the torsional angle of the C=O bond with respect to the C=C bond which determines the sign of the rotatory strength in the excited state.

The computational results support in principle this conclusion, but enable us to shed some more light on the observed CPL spectra. According to the DFT results, two of the enones studied (**1a** and **2**) have only one excited-state structure. For these systems, the calculated sign of the CPL dissymmetry factor g_e is in agreement with experiment (same as the CD sign in the case of **1**, opposite for **2**), and it is correctly predicted

Table 2 Experimental and calculated (CAM-B3LYP/aug-cc-pVDZ) spectroscopic parameters for the $n \rightarrow \pi^*$ and $n \leftarrow \pi^*$ transitions. aug-cc-pVDZ basis set

	Exp.	Calc., **G**	Exp.	Calc., **E1**	Calc., **E2**
Dissymmetry factor g (10^{-3})					
1	17.8	31.2	−6.3	16.1	−11.9
1a	5	6.5	−12	—	−16.5
2	56.8	69.8	29.4	—	45.9
3	45.8	57.4	15.7	47.8	−2.1
4	−32.5	−52.6	<3	−26.2	4.3
Rotatory strength R (10^{-40} cgs)					
1	6.22	8.54	—[a]	5.72	−9.86
1a	6.29	6.79	—	—	−35.71
2	51.10	45.57	—	—	30.96
3	20.50	21.92	—	13.40	−1.62
4	−15.20	−18.61	—	−9.19	3.30
Dipole strength D (10^{-40} cgs)					
1	1400	1097	—	1418	3306
1a	5090	4159	—	—	8677
2	3600	2612	—	—	2699
3	1790	1527	—	1122	3095
4	1870	1415	—	1404	3045
Vertical transition energy ΔE/eV					
1	≈4.1[b]	4.24	—	2.77	2.91
1a	≈4.1[b]	4.21	—	—	2.81
2	≈4.1[b]	4.18	—	—	2.86
3	≈4.1[b]	4.24	—	2.96	2.96
4	≈4.1[b]	4.23	—	2.31	2.52

[a] No experimental results available. [b] Schippers, van der Ploeg and Dekkers[4] give only the approximate position of the absorption bands.

that the emission dissymmetry factor g_e of **2** is smaller than its absorption dissymmetry factor g_a. Three of the enones studied have instead two excited-state structures (denoted **E1** and **E2**) with opposite signs for the rotatory strengths. Comparison of the sign of the CPL intensity with experiment indicates that for **1** the **E2** structure is the most populated one, for **3** it is the **E1** structure, and for **4** it is the **E2** structure. This is in agreement with the energy ordering obtained using the CAM-B3LYP functional (but this is not the case for B3LYP for molecules **1** and **4**).

Assuming the CAM-B3LYP predictions of the excited-state energy ordering to be correct, the worst agreement between theory and experiment for the emission g factor is observed for molecule **3**: the experimental value is approximately three times smaller than the calculated one. The possible sources of this and other discrepancies will be discussed later.

2 Electron correlation and basis set effects

a. Comparison of CAM-B3LYP and B3LYP results. The influence of the use of a Coulomb-attenuated exchange–correlation functional on the calculated spectra of β,γ-enones in their ground and excited states is illustrated by a comparison of the CAM-B3LYP and B3LYP results (see Table 3).

The largest influence of moving from the B3LYP to the CAM-B3LYP functional is observed in the case of the dipole strengths—the B3LYP results tend to be a factor of 2 larger than the CAM-B3LYP ones. In all cases except molecule **2**, the CAM-B3LYP result is much closer to the experimental one

(see Table 2). The comparison with available experimental data (those for the CD spectra) indicates that the same is true of the rotatory strengths.

In the case of the dissymmetry factors, the B3LYP results are actually closer to the experiment than the CAM-B3LYP ones, but this is caused by an accidental cancellation of errors in the rotatory and dipole strengths. Generally, the DFT dissymmetry factors are in satisfactory agreement with the experiment, except for molecule **3**, where the computational result for the fluorescence g_e factor is, independently of the choice of exchange–correlation functional, much overestimated in comparison to the experiment. The reason for this is not clear: it does not seem to stem from an error in the electron density description, since the other results (including those for the absorption in molecule **3**) are in far better agreement with the experiment, as already demonstrated. Enlargement of the basis set affects the results very little (see below), so the incompleteness of the basis set is a very unlikely source of error. It is more likely that the overestimation originates in an incorrect prediction of the excited-state geometry. We will return to this issue in the following part of the paper.

b. Comparison of CC2 and DFT results. The ground- and excited-state spectroscopic parameters of the smallest enone, molecule **2**, have also been calculated at the CC2 level. The rotatory and dipole strengths calculated for **2** using CC2 (at the B3LYP geometry to allow for a more direct comparison with the DFT data) are listed in Table 4, together with the DFT results. We have also in this table listed the numbers obtained using the velocity- and length-gauge approaches. As one can see, the velocity- and length-gauge results are similar in the case of DFT, but they differ significantly for CC2. This is understandable, considering that in the case of CC2 not only the incompleteness of a basis set but also the truncation of the CC expansion contributes to this difference. This makes the comparison of the CC2 and DFT results rather difficult. The CC2 and CAM-B3LYP rotatory strengths seem to be close to each other, and so are the dipole strengths (at least when the mixed-gauge results are compared). The B3LYP results are overestimated in comparison to them, both the rotatory and dipole strength. The CC2/aug-cc-pVDZ vertical excitation energy is 4.25 eV, to be compared with 4.18 eV obtained using CAM-B3LYP and 4.03 eV obtained using B3LYP. The CAM-B3LYP result is thus closer to the CC2 one, as was also the case for the transition moments.

c. Basis-set effects. Table 5 contains the dipole and rotatory strengths calculated for the $n \rightarrow \pi^*$ transition of the ground-state structures using different basis sets. We have also performed calculations for the excited-state structures, but the trends are similar, so we do not tabulate these data.

The rotatory and dipole strengths depend little on the choice of basis set in the series of augmented correlation-consistent basis sets. The addition of the second set of diffuse functions (extension from aug-cc-pVDZ to daug-cc-pVDZ) leaves the results practically unaffected (as expected for a valence transition). The extension from aug-cc-pVDZ to aug-cc-pVTZ increases the absolute value of the rotatory strength for all systems studied by less than 2%, in one case (molecule **2**) decreasing, in most cases increasing the difference between computed and experimental results. The dipole strengths are underestimated at the CAM-B3LYP/aug-cc-pVDZ level and the extension from the aug-cc-pVDZ to the aug-cc-pVTZ basis set increases their values, improving the agreement between the calculated and experimental results.

Another test of the completeness of the basis set for the calculations of the rotatory strengths is a comparison of the results obtained in the length gauge with and without the use of London orbitals. The differences (not shown in Table 5) amount to about 0.5% for aug-cc-pVDZ and 0.1% for aug-cc-pVTZ, except for molecule **2**, for which the discrepancy

Table 3 Comparison of the CD parameters obtained using the B3LYP and CAM-B3LYP functionals and aug-cc-pVDZ basis set

	Ground state **G**		Excited state **E1**		Excited state **E2**	
	CAM-B3LYP	B3LYP	CAM-B3LYP	B3LYP	CAM-B3LYP	B3LYP
Dipole strength D (10^{-40} cgs)						
1	1097	2401	1418	1213	3306	4356
1a	4159	9902	—	—	8677	14690
2	2612	4344	—	—	2699	3905
3	1527	2921	1122	1216	3095	4179
4	1415	3037	1404	1205	3045	3926
Rotatory strength R (10^{-40} cgs)						
1	8.54	13.51	5.72	7.87	−9.86	−11.73
1a	6.79	8.70	—	—	−35.71	−47.76
2	45.57	57.81	—	—	30.96	33.27
3	21.92	30.13	13.40	19.01	−1.62	−0.59
4	−18.61	−26.14	−9.19	−13.05	3.30	2.62
Dissymmetry factor g (10^{-3})						
1	31.2	22.5	16.1	25.9	−11.9	−10.8
1a	6.5	3.5	—	—	−16.5	−13.0
2	69.8	53.2	—	—	45.9	34.1
3	57.4	41.3	47.8	62.5	−2.1	−0.6
4	−52.6	−34.4	−26.2	−43.3	4.3	2.7

Table 4 Comparison of the rotatory and dipole strengths of **2** calculated at various levels of theory using the aug-cc-pVDZ basis set

	2G	**2E**
Rotatory strength R (10^{-40} cgs)		
CC2 *length gauge*	48.91	28.58
CC2 *velocity gauge*	41.91	21.54
B3LYP *length gauge*, GIAO	57.81	33.27
B3LYP *length gauge*	56.32	31.32
B3LYP *velocity gauge*	55.86	30.33
CAM-B3LYP *length gauge*, GIAO	45.57	30.96
CAM-B3LYP *length gauge*	44.06	26.95
CAM-B3LYP *velocity gauge*	43.83	26.37
Exp.	51.1	—
Dipole strength D (10^{-40} cgs)		
CC2 *length gauge*	3243	3602
CC2 *velocity gauge*	2394	2265
CC2 *mixed gauge*	2512	2979
B3LYP *length gauge*	4344	3905
B3LYP *velocity gauge*	4228	4011
B3LYP *mixed gauge*	4285	3951
CAM-B3LYP *length gauge*	2612	2699
CAM-B3LYP *velocity gauge*	2541	2851
CAM-B3LYP *mixed gauge*	2576	2768
Exp.	3600	—

Table 5 Dependence of the calculated CD spectroscopic parameters for the $n \rightarrow \pi^*$ excitation on the basis set. CAM-B3LYP functional

	1	1a	2	3	4
Rotatory strength R [10^{-40} cgs]					
aug-cc-pVDZ	8.50	6.76	44.06	21.86	−18.53
daug-cc-pVDZ	8.48	6.78	43.98	21.86	−18.59
aug-cc-pVTZ	8.55	—	44.61	21.95	−18.83
Exp.[a]	6.22	6.29	51.10	20.50	−15.20
Dipole strength D [10^{-40} cgs]					
aug-cc-pVDZ	1097	4159	2612	1527	1415
daug-cc-pVDZ	1096	4156	2606	1522	1413
aug-cc-pVTZ	1124	—	2668	1541	1450
Exp.[a]	1400	5090	3600	1790	1870

[a] Schippers, van der Ploeg and Dekkers.[4]

is about 3%, probably because of the small size of the system. It therefore does not seem likely that the size of the basis set is a significant source of error in the calculations of the rotatory strengths.

As far as the dipole strengths are concerned, the extension of the basis set from aug-cc-pVDZ to aug-cc-pVTZ increases their magnitudes (to the same extent as in the case of the rotatory strengths), while the addition of a second set of diffuse functions has very little influence on the results.

3 Rotatory strength as a function of geometric parameters. The largest changes in geometry of the β,γ-enones upon $n \rightarrow \pi^*$ excitation is the puckering of the carbonyl group and the elongations of the C═O and C═C bonds. The differences in the rotatory strength for the two excited-state structures indicate that the first factor is crucial in determining the appearance of the first band in the ECD and CPL spectra, but in order to further elucidate the role of the individual parameters, we have carried out additional calculations with the selected geometric parameters changed systematically. We have chosen molecules **3** and **4** for these investigations, since the largest discrepancy between the calculated and experimental results was observed for **3**, and **4** is structurally very closely related (it is an isomer of **3**, with the C═CH_2 and C═O groups exchanged).

The first set of calculations have been carried out for molecules **3** and **4**, where the θ(═C–C–C═O) dihedral angle has been changed from the values corresponding to the **3E1** and **4E1** structures (184.3° and 170.1°, respectively) to those corresponding to the **3E2** and **4E2** structures (106.8° and 75.0°, respectively). (For the ground-state structures **3G** and **4G**, the dihedral angles are 150.1° and 127.5°, respectively.) The results are displayed in Fig. 3. One can observe that the position of the C═O bond with respect to the remaining part of the molecule (here expressed as the θ(═C–C–C═O) dihedral angle instead of ϕ(C═O···C═C) for convenience, even though both angles were changed simultaneously) is indeed the most important parameter governing the sign and magnitude of the $n \rightarrow \pi^*$ rotatory strength, and that the dependence is regular and periodic. The shape of the curve is practically independent of the other geometric parameters (compare **3E1** and **3E2** or **4E1** and **4E2** curves), and similar

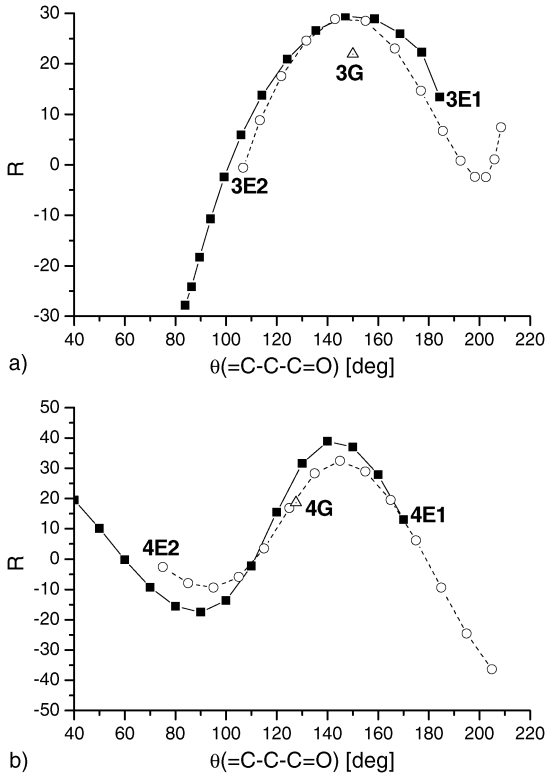

Fig. 3 The dependence of the $n \rightarrow \pi^*$ rotatory strength (B3LYP/aug-cc-pVDZ results) in the molecules **3** and **4** on the θ(═C–C–C═O) dihedral angle, with the remaining geometry parameters kept at their values for **3E1**, **3E2** (graph a), **4E1** and **4E2** (graph b) structures, respectively.

for both molecules: the curves are shifted with respect to each other, but only slightly rescaled.

The results corresponding to the minima **3E1** and **3E2** (and also **4E1**) are located where the slope of the dependence on the conformation is very steep. Thus, even a small error in the dihedral angle can propagate into the rotatory strength, causing a large error in the final value of the dissymmetry factor. This can explain, at least partly, the discrepancy between theory and experiment observed for the CPL intensity of molecule **3**.

The graphs in Fig. 3 also display the $n \rightarrow \pi^*$ rotatory strengths calculated for the ground-state structures of molecules **3** and **4**. One can observe that their magnitudes are smaller than for the excited-state-like geometries with only the θ(═C–C–C═O) dihedral angle set to the value corresponding to the ground state structures (continuous curves), which indicates that there are other geometric parameters than the dihedral angle governing this parameter. In order to elucidate this, we have carried out calculations for the ground-state-like structures (**3G** and **4G**), changing only the C═O and C═C bond lengths to the values corresponding to the excited-state structures.

The results of this set of calculations are displayed in Fig. 4. The changes in the rotatory strengths with bond elongation are less dramatic than in the case of the C═O group puckering, but nevertheless non-negligible. Interestingly, they have an opposite effect and partially cancel each other: elongation of

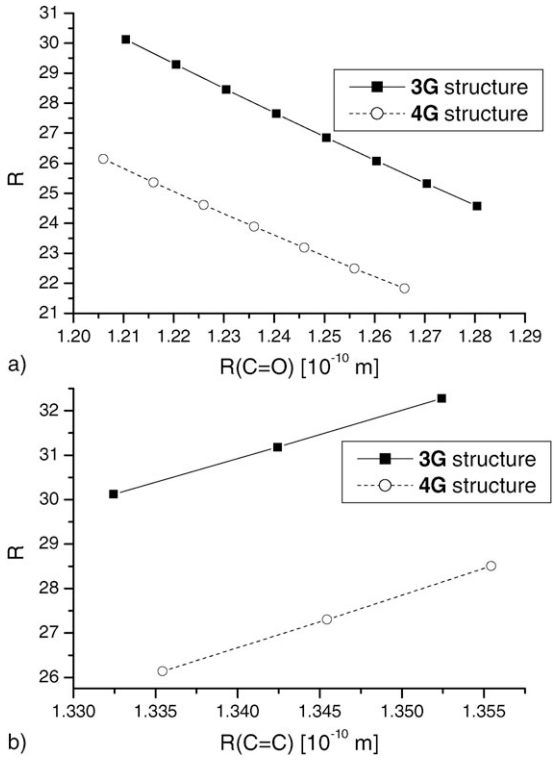

Fig. 4 The dependence of the $n \rightarrow \pi^*$ rotatory strength (B3LYP/aug-cc-pVDZ results) in the molecules **3** and **4** on the *R*(C═O) (graph a) and *R*(C═C) (graph b) bond lengths, with the remaining geometry parameters kept at their values for **3G** and **4G** structures, respectively.

the C═O bond causes decrease in the rotatory strength (Fig. 4a) while elongation of the C═C bond causes it to increase (Fig. 4b). The slope of the dependence is, rather surprisingly, larger in the case of the changes of the C═C bond length than for the C═O bond length. The origin of this phenomenon is not certain, but it may be connected with the fact that the orbitals involved in the $n \rightarrow \pi^*$ excitation, although formally belonging to the carbonyl group, are to some extent delocalized on the C═C moiety. (The exciton coupling effect between the $n \rightarrow \pi^*$ transition and the first transition of the C═C chromophore can be expected to be negligible[27] and not to contribute to this effect, since the energy difference between the two transitions is large.)

As noted before, B3LYP tends to underestimate the C═O bond length in the excited state, so this may be part of the reason why the calculated emission dissymmetry factors (especially for **3**) are overestimated in comparison to the experiment. It should be also taken into account that our calculations have been carried out in the Born–Oppenheimer approximation with complete neglect of vibronic coupling, which is likely to be a substantial source of error, especially considering the large change of geometry observed between the ground and excited state.

IV. Summary and conclusions

The circularly polarized luminescence (CPL) and electronic circular dichroism (CD) spectroscopic parameters corresponding to the $n \leftarrow \pi^*$ and $n \rightarrow \pi^*$ transitions, respectively, have been calculated for selected β,γ-enones using density functional response theory. The coupled-cluster response method (at the CC2 level) has been used for the smallest system for comparison. The investigation was motivated by the experimental work of Schippers *et al.*,[4] who demonstrated that for some of the enones, the sign of the CD and CPL bands are different. They attributed this to the puckering of the carbonyl group in the excited state, stating that it can tilt either towards the C═C double bond or in the opposite direction, causing an inversion of the CPL band with respect to the CD band. Our results support in principle this conclusion, but they also show that for three of the five enones studied there exists not only one, but two excited-state minima, and that their relative energies influence the sign of the CPL band. In all cases studied, the calculated signs of the CD and CPL bands are in agreement with the experiment when the CAM-B3LYP exchange–correlation functional is used for the energy ordering of the excited-state structures.

Acknowledgements

The work has been financed by the Ministry of Science and Higher Education (Poland) from funds for scientific research in years 2009–2011 as project No. N N204 138637. The work has also received support from the Research Council of Norway through a Centre of Excellence grant (Grant No. 179568/V30) as well as Grants No. 191251 and 177558/V30. This work has also received support from the Norwegian Supercomputing program and Wroclaw Centre for Networking and Supercomputing through a grant of computer time.

References

1 H. M. Brittain, *Chirality*, 1996, **8**, 357.
2 H. Tsukube and S. Shinoda, *Chem. Rev.*, 2002, **102**, 2389.
3 H. P. J. M. Dekkers and L. E. Closs, *J. Am. Chem. Soc.*, 1976, **98**, 2210.
4 P. H. Schippers, J. P. M. van der Ploeg and H. P. J. M. Dekkers, *J. Am. Chem. Soc.*, 1983, **105**, 84.
5 P. H. Schippers and H. P. J. M. Dekkers, *J. Am. Chem. Soc.*, 1983, **105**, 145.
6 P. Sałek, O. Vahtras, T. Helgaker and H. Ågren, *J. Chem. Phys.*, 2002, **117**, 9630.
7 F. Furche and R. Ahlrichs, *J. Chem. Phys.*, 2002, **117**, 7433.
8 J. Olsen and P. Jørgensen, *J. Chem. Phys.*, 1985, **82**, 3235.
9 K. L. Bak, A. E. Hansen, K. Ruud, T. Helgaker, J. Olsen and P. Jørgensen, *Theor. Chim. Acta*, 1995, **90**, 441.
10 F. London, *J. Phys. Radium*, 1937, **8**, 397.
11 W. Koch and M. C. Holthausen, *A Chemist's Guide to Density Functional Theory*, Wiley-VCH, Weinheim, 2001.
12 M. J. G. Peach, T. U. Helgaker, P. Salek, T. W. Keal, O. B. Lutnaes, D. J. Tozer and N. C. Handy, *Phys. Chem. Chem. Phys.*, 2006, **8**, 558.
13 M. J. G. Peach, P. Benfield, T. U. Helgaker and D. J. Tozer, *J. Chem. Phys.*, 2008, **128**, 044118.
14 T. Yanai, D. P. Tew and N. C. Handy, *Chem. Phys. Lett.*, 2004, **91**, 551.
15 O. Christiansen, H. Koch and P. Jørgensen, *Chem. Phys. Lett.*, 1995, **243**, 409.
16 A. Köhn and C. Hättig, *J. Chem. Phys.*, 2003, **119**, 5021.
17 T. H. Dunning, *J. Chem. Phys.*, 1989, **90**, 1007.
18 R. A. Kendall, T. H. Dunning and R. J. Harrison, *J. Chem. Phys.*, 1992, **96**, 6796.
19 D. E. Woon and T. H. Dunning, *J. Chem. Phys.*, 1993, **98**, 1358.

20 D. E. Woon and T. H. Dunning, *J. Chem. Phys.*, 1994, **100**, 2975.
21 M. Pecul, K. Ruud and T. Helgaker, *Chem. Phys. Lett.*, 2004, **388**, 110.
22 Dalton, a molecular electronic structure program, release 2.0 (2005), see http://www.kjemi.uio.no/software/dalton/dalton.html.
23 R. Ahlrichs, M. Bär, M. Häser, H. Horn and C. Kölmel, *Chem. Phys. Lett.*, 1989, **162**, 165.
24 V. A. Job, V. Sethuraman and K. K. Innes, *J. Mol. Spectrosc.*, 1969, **30**, 365.
25 P. Jensen and P. R. Bunker, *J. Mol. Spectrosc.*, 1982, **94**, 114.
26 P. H. Schippers and H. P. J. M. Dekkers, *J. Am. Chem. Soc.*, 1983, **105**, 79.
27 N. Harada and K. Nakanishi, *Circular Dichroic Spectroscopy—Exciton Coupling in Organic Stereochemistry*, University Science Books, Mill Valley, CA, 1983.

